ORIGINAL RESEARCH

High-performance conductive adhesives based on water-soluble resins for printed circuits, flexible conductive films, and electromagnetic interference shielding devices

Ge Cao[1] · Shaoyong Cai[1] · He Zhang[2] · Yanqing Tian[1]

Abstract

Herein, we report high-performance electrically conductive adhesives (ECAs) as promising materials for flexible conductive films, printed circuits, and electromagnetic interference shielding devices. Through combining a small amount of water-dispersible polyaniline (PANI) nanorods and silver flakes into water-based polyurethane (WPU), the obtained ECAs showed high electrical conductivity with a low Ag content (4.8×10^4 S/cm, 60 wt% of silver, and 6% PANIs) and excellent stability; this stability withstood aging without change at 85 °C/65% RH for at least 20 days. Prototyped applications of the ECAs for flexible conductive films, printed circuits, and electromagnetic interference shielding devices were demonstrated. When these ECAs were used as flexible conductive films, these films exhibited excellent electrical performance under high mechanical deformation. The resistance of films remained unchanging after being bent with a 6-mm radius for over 8000 cycles, applied with 1000 kPa pressure, or stretched 20% for over 1000 cycles. The printed circuits had excellent flexibility and good adhesion on flexible substrates, enabling the circuits' stable operation at a high deformation. Moreover, novel conductive foams with high conductivity of 283.4 S/m and reasonable electromagnetic interference shielding effectiveness (EMI SE) of above 34 dB were obtained by integrating the ECAs with PU sponges to broaden the applications of ECAs. Therefore, this study provided an original, uncomplicated, low-price route to fabricate high-performance ECAs based on water-soluble resins for various flexible electronic devices.

Keywords Water-dispersible polyaniline · Electrically conductive adhesives · Flexible conductive films · Printed circuits · Electromagnetic interference shielding

1 Introduction

In the dawn of highly available smart electronic products and the growing demand for environment-friendly production systems, electrically conductive adhesives (ECAs) have become increasingly important, which could provide cost-effective and straightforward tools for various flexible electronic devices [1, 2]. ECAs, a kind of polymer composite materials with conductive fillers, have numerous advantages, such as low treatment temperatures, high printing resolutions, and excellent compatibility with conventional printing methods [3–6]. Although they possess many benefits, some shortcomings still need to be addressed to meet the future needs of the booking flexible electronic market. These obstacles lie mainly the use of large amounts (70–80%) of metal fillers (such as Ag micro-flakes, which are used widely in ECAs due to their excellent electrical conductivity and chemical stability) to maintain the conductivity of ECAs. The use of large amount of metal fillers can damage the adhesion of ECAs and raise the cost [7, 8]. In addition, toxic diluents such as 1,4-dioxane used in the manufacture of ECAs also become a severe problem for human health [9, 10]. Therefore, the development of water-based and high-performance ECAs with low silver contents has become a top priority.

To improve electrical performances and reduce the cost of ECAs, various methods have been proposed. For example, conducting-enhancers such as carbon materials [11–15] and

✉ Yanqing Tian
tianyq@sustech.edu.cn

1   Department of Materials Science and Engineering, Southern University of Science and Technology, Shenzhen 518055, China

2   State Key Laboratory of Advanced Welding and Joining, Harbin Institute of Technology, Harbin 150001, China

conducting polymer nanomaterials [10, 16–19] have been added to Ag-filled ECA formulations to bridge metal fillers to improve the ECAs' conductivity effectively. Nano-scale silver fillers (Ag particles, Ag nanowires) enable the sintering of metal fillers to reduce the contact resistance of ECAs [8, 20–24]. Chemical treatment of metal fillers to improve quality is also a general method to increase the electrical performance of ECAs [25–27]. Although significant progress has been made in elevating the conductivity of ECAs, designing high-performance ECAs with water-soluble resins such as water-based PU is challenging due to the insolubility of most conducting-enhancers such as carbon materials and conducting polymers in water and water-soluble resins.

To address the above challenges, we presented a facile strategy to synthesize a kind of water-dispersible polyaniline nanorods (PANI nanorods) with high conductivity and zeta potential (49 mV), which could form stable conductive colloids in aqueous solutions [28]. These characteristics made PANI nanorods well dispersed in the water-soluble resin (water-based PU) and connected the gaps among silver flakes to improve electrical performances of ECAs significantly. Compared with other conductive polymers, PANI has become the most explored material owing to its fascinating low manufacturing price, excellent chemical stability, and adjustable conductivity [29–38]. However, as far as we know, the synthesis and use of water-dispersible PANI nanorods as conducting-enhancers for achieving outstanding electrical conductivity of ECAs with the reduced amounts of metal fillers were seldomly reported. Moreover, the ECAs were first-time applied in the manufacture of electromagnetic interference shielding devices to reduce electromagnetic pollution. Herein, we presented the remarkable enhancement in the electrical performances of ECAs by adding small amounts of water-dispersible PANI nanorods. These PANI could serve as conductive interconnections among Ag flakes of ECAs to reduce the contact resistance significantly. Thus, a kind of new ECAs based on water-soluble resins was successfully prepared. Furthermore, prototyped applications of the ECAs for flexible conductive films, printed circuits, and electromagnetic interference shielding devices were explored, which showed potential applications of the new ECAs for various flexible electronic devices.

2 Experimental

2.1 Materials

Ethanol (C_2H_5OH), dioxane ($C_4H_8O_2$), methyl isobutyl ketone ($CH_3C(=O)CH_2CH(CH_3)_2$), ethyl acetate ($CH_3COOC_2H_5$), methanol (CH_3OH), n-hexane ($CH_3(CH_2)_4CH_3$), and acetone (CH_3COCH_3) were supplied by Beijing Yinuokai Technology Co., Ltd. (Beijing, China). Ammonium persulfate (APS), poly(N-Vinylpyrrolidone) (PVP, K10), potassium bromide (KBr), methyl orange (MO), and aniline hydrochloride (C_6H_8ClN) were supplied by Adamas Reagent Co., Ltd. (Shanghai, China). Water-based polyurethane (WPU) was purchased from Shenzhen Yoshida Chemical Co., Ltd. (Shenzhen, China). The Ag powder (flake morphology) was purchased from Lijia Metal Materials Co., Ltd. (Changsha, Hunan). Electronic components (resistors, capacitors, LEDs) were provided by Changzhou Qiguang Lighting Co., Ltd. (Changzhou, China).

2.2 Synthesis of water-dispersible PANI nanorods

Water-dispersible PANI nanorods were synthesized by classical oxidative polymerization of aniline in water. First, MO (0.37 g) was dissolved in 150 mL of PVP solution (0.05%) in a 200-mL beaker. Next, 1.30 g of aniline hydrochloride was then dispersed in the solution with vigorous agitation for 60 min at 25 °C. Then, 50 mL of an APS aqueous solution (10 mmol) was poured into the above mixture under vigorous stirring to polymerize aniline. Twenty-four hours later, the formation of dark green color precipitation confirmed the successful polymerization of aniline. The PANI nanorods with 80% yield were filtered and rinsed with dilute HCl solutions (1 mol/L) several times.

As a comparison, conventional PANI particles were obtained based on Stejskal's previous work [39]. The PANI particles were synthesized by the oxidation of 0.2 mmol aniline hydrochloride with 0.25 mmol APS in 200 mL deionized water at 25 °C.

2.3 Preparation of PANIs/WPU nanocomposites and ECAs

PANI nanorods/WPU and PANI particles/WPU nanocomposites were prepared by dispersing certain amounts of PANI nanorods or PANI particles into 0.5 g water-based PUs. The nanocomposites were obtained after the evaporation of water in the mixtures.

To evaluate the effect of PANI nanorods on ECAs' performance, two types of ECAs were prepared (Table 1). One type is with PANIs (the WPN series); another type is without PANIs (the WPU series). A detailed fabricating process for WPN-2 was provided as an example. Firstly, PANI nanorods (0.12 g) were dispersed to 8 mL of deionized water in a 50-mL beaker by ultrasonic treatment for 30 min. Secondly, 1 g water-based PUs was added to the suspension. Next, Ag micron-flakes (1.35 g) were poured into the mixture under vigorous stirring. Finally, the paste-like ECAs composing PANI nanorods were obtained by eliminating excess water in the beaker.

Table 1 The components of the prepared ECAs

Sample code	WPU resin (wt%)	Ag content (wt%)	PANI nanorods (wt%)	Curing temperature (°C)
WPN-1	44	50	6	25
WPN-2	34	60	6	25
WPN-3	24	70	6	25
WPN-4	39	60	1	25
WPN-5	38	60	2	25
WPN-6	36	60	4	25
WPN-7	42	60	8	25
WPN-8	34	60	6	25
WPN-9	34	60	6	120
WPN-10	34	60	6	180
WPU-1	50	50	0	25
WPU-2	40	60	0	25
WPU-3	30	70	0	25
WPU-4	40	60	0	200

Notice: the ECAs composed of silver flakes and PANI nanorods were called the WPN series; the ECAs containing silver flakes only were called the WPU series

2.4 Fabrication of electronic devices with ECAs

The flexible conductive film was fabricated by the casting method. Twenty-milliliter WPN-2 ECAs were poured onto a rectangular mold ($100 \times 50 \times 2$ mm) to evaporate solvent at 80 °C for 2 h on a heater. The printed circuit with a line width of 2 mm was made by screen printing onto a flexible PDMS substrate using WPN-2 ECAs.

The conductive ECAs@PU foam was fabricated with a dip-coating technique. A PU foam ($20 \times 20 \times 5$ mm) was initially immersed in the 100 mL WPN-2 ECAs by sonication for 20 min. With the continuous deposition of the ECAs, the color of PU foam changed to silver-brown. Next, the ECAs-modified PU foam was repeatedly immersed in ECA under ultrasonic treatment for different cycles. Finally, the ECAs-modified PU foam was dried at 80 °C for 4 h to obtain a silver-gray ECAs@PU foam.

2.5 Characterization methods

The morphologies and sizes of the water-dispersible PANI nanorods, Ag micron-flakes, PANI nanorods' distribution in ECAs, and the ECAs-modified PU sponge were investigated by a scanning electron microscope (SEM, MIRA3, TESCAN, Czech). The dispersibility of the water-dispersible PANI nanorods in water was measured by the dynamic light scattering (DLS) method with a Malvern Zetasizer Nano ZS (Worcestershire, UK). The samples (0.01 g of PANI nanorods in 20 mL water) to be analyzed in DLS were filtrated through a 0.8-µm PTFE filter.

A typical dispersibility experiment was carried out in various organic solvents. First, 0.01 g of PANI nanorods were dispersed into 20 mL of the selected solvents (ethanol, dioxane, methyl isobutyl ketone, ethyl acetate, methanol, n-hexane, and acetone). After leaving the sample at 25 °C for 4 h, a photograph of the suspension was taken.

The electrical conductivity of PANI nanorods was determined by a four-point probe system (RTS-9, 4 PROBES TECH, Guangzhou, China). PANIs were compressed into dense pellets for conductivity measurements.

The electrical performance of the ECAs was measured by the above four-point probe system, which was consistent with our previously published procedure [11]. Briefly, the viscous samples were dropped into a rectangular mold and flattened to generate ECAs films (length 80 mm, width 40 mm, height 50 µm). Subsequently, these films were heated at selected temperatures for 2 h before the conductivity measurement.

The ECAs-modified PU sponge's conductivity was determined by a two-point measurement with a multimeter (ZTY890D, TaiDe, China). Rectangle samples ($20 \times 60 \times 5$ mm) were used for electrical analysis. The measured volume resistance (Ω), R, was converted to volume resistivity, ρ, using the formula $\rho = R*A/L$. A is the active sectional area of the conductor, and L is the length of the conductor.

The infrared spectrum of PANI nanorods was determined with a Fourier transform infrared (FT-IR) spectrometer (Waltham, USA). The samples were mixed with KBr powder and then compacted into a pellet for FT-IR measurement.

A conductive film ($100 \times 10 \times 0.5$ mm) produced from the above ECAs was screen printed onto flexible polymer substrates (PDMS) for the bending test. A specialized stretching system (detailed in Fig. S1) was used to measure the films' resistance change with different bending radius, and the running speed is 20 mm/min.

The tensile test of the conductive film ($100 \times 10 \times 0.5$ mm) made by the casting methods was conducted by using the above-specialized stretching system. The pressure test using the same film was conducted on a pressure device.

The EMI SE of the foams was evaluated in the X band ($9-18$ GHz) using a vector network analyzer (PNA E5227B). All samples were sliced into rectangular slices ($5 \times 10 \times 22.78$ mm) for electromagnetic interference shielding tests in the X band. EMI SE was calculated by the equations S1–S6 in supporting information.

3 Results and discussion

3.1 The preparation of ECAs

Figure 1a, b show a diagrammatic sketch of fabricating high-performance ECAs with the water-dispersible PANI

nanorods. Highly dispersible PANI nanorods are prepared by typical oxidative polymerization of aniline hydrochloride with the help of the methyl orange (MO). These PANI nanorods and silver micro flakes were dispersed in the water-based PU resin to prepare the high-performance ECAs. The prepared ECAs were used to manufacture flexible conductive films, printed circuits, and electromagnetic interference shielding devices. Figure 1c shows a diagrammatic sketch of the conductive films produced by the ECAs. Figure 1d shows a diagrammatic illustration of manufacturing flexible printed circuits. Figure 1e shows a diagrammatic illustration of high-performance electromagnetic interference shielding devices by dipping the ECAs into a commercial PU foam.

3.2 Characterizations of water-dispersible PANI nanorods

The morphologies of PANI nanorods are given in Fig. 2a. It is seen that the PANI nanorods exhibited rod-shaped morphologies with a relatively uniform length distribution.

The lengths of the nanorods range from 2 to 5 μm. Their diameters are about 100–300 nm. This result is very different from the traditional synthesis of PANI particles without methyl orange (MO), which shows the aggregated globular morphologies (200 nm) in Fig. S2. Generally, spherical nanoparticles are unfavorable relative to nanotube morphology for conductive studies [40, 41]. Therefore, the construction of nanotubular PANI materials could improve conductivity.

The infrared spectrum of PANI nanorods is investigated by FT-IR measurement. The central IR band of PANI is given in Fig. 2b, which agrees with previous reports [42]. The IR bands about 3407 cm^{-1} and 3120 cm^{-1} are ascribed to the N–H stretching mode of PANIs. The absorption peaks observed at 1314 cm^{-1} and 1290 cm^{-1} are C$=$C stretching vibration for quinoid and benzenoid rings. The peak at 1107 cm^{-1} belongs to the C–N stretching mode for the benzenoid ring. Other vibrations of the C-H plane bending vibrations emerged around 621 cm^{-1}.

The formation mechanism of PANI nanorods is explained in Fig. 2c. Well-soluble MO salt could convert into a poorly
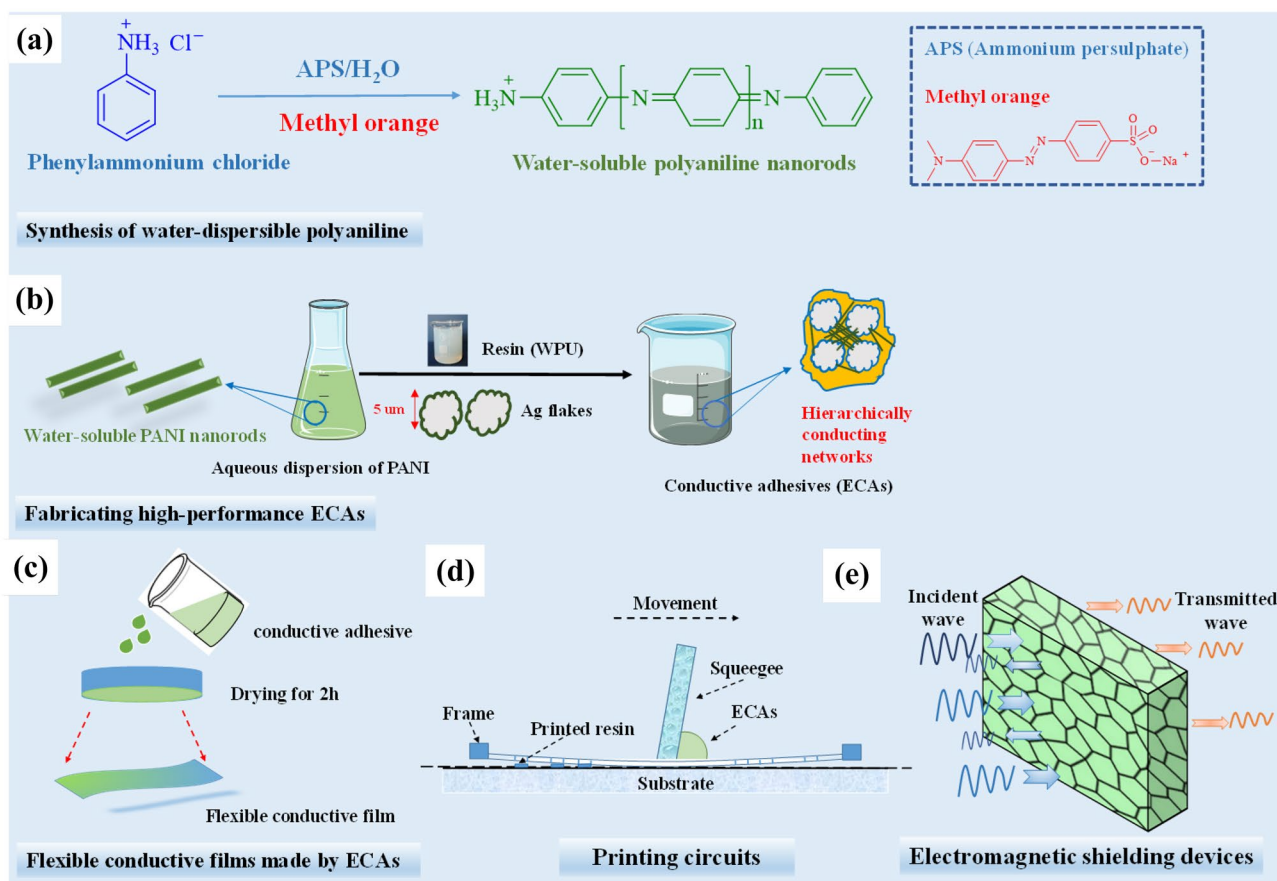

Fig. 1 (**a**) Diagrammatic sketch showing the synthesis of water-dispersible PANI nanorods. (**b**) Diagrammatic sketch showing fabricating high-performance ECAs based water-soluble resin. (**c**) Diagrammatic sketch of the conductive films produced by ECAs. (**d**) Diagrammatic illustration of manufacturing flexible printed circuits. (**e**) Diagrammatic illustration of electromagnetic interference shielding devices by dipping the ECAs into a commercial PU foam
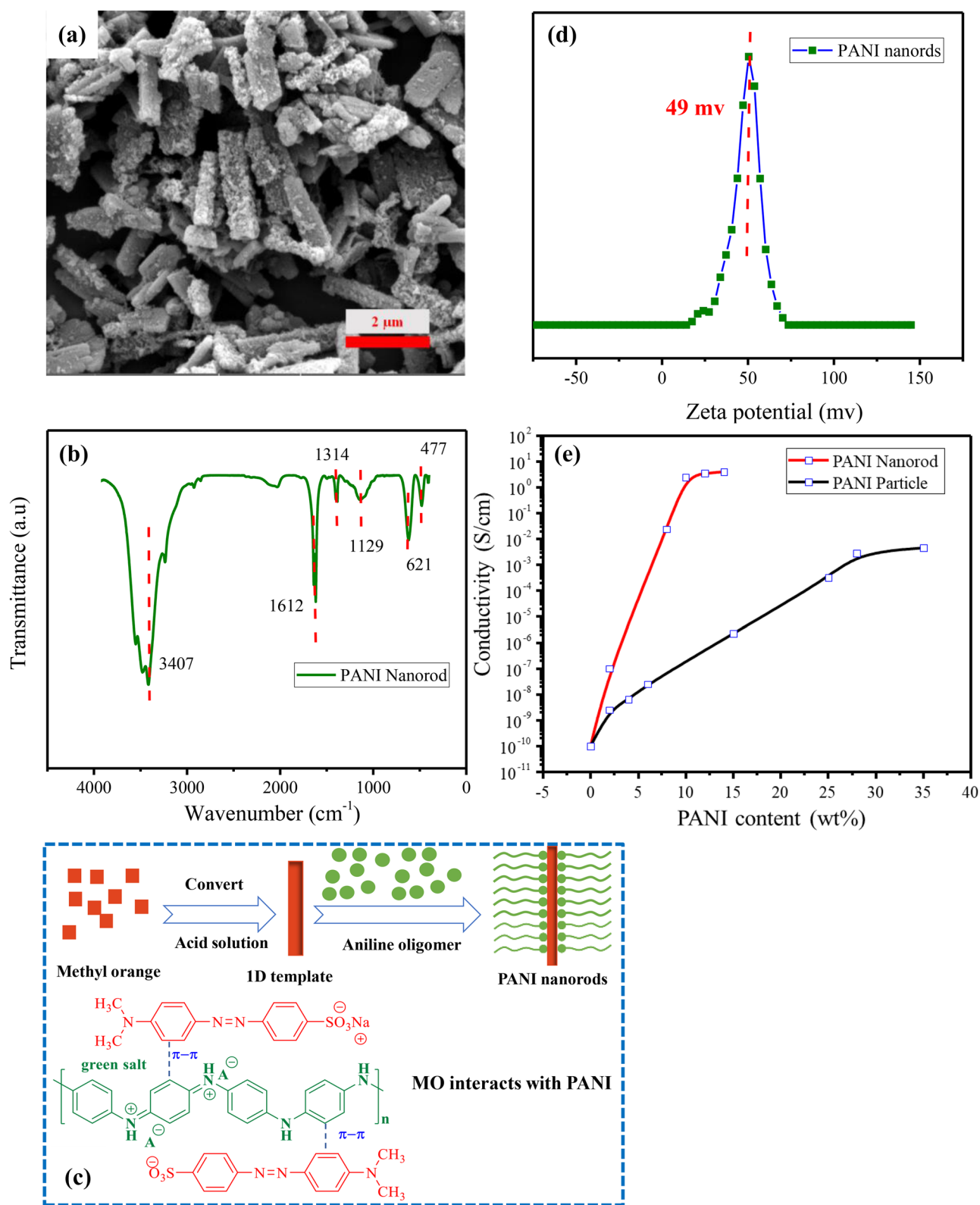
Fig. 2 **a** The morphologies of PANI nanorods. **b** The IR spectrum of PANI nanorods. **c** The formation mechanism of PANI nanorods. **d** The Zeta potential of PANI nanorods. **e** The conductivity of PANI nanorods/WPU and PANI particles/WPU nanocomposites as a function of PNAI loading

soluble acidic form as a hydrophilic one-dimensional (1D) template at pH 3–4, which is achieved after adding acidic aniline hydrochloride. The aggregation of the rigid rod molecules of methyl orange acid leads to a hydrophilic 1D template in aniline polymerization [43, 44]. Finally, the aniline is polymerized at its surface by π–π interactions between the aromatic rings of MO and constitutional polymer units. Thus, highly conducting and water-dispersible PANI nanorods were successfully synthesized in the presence of methyl orange.

The suspension characteristics of PANI nanorods are displayed in Fig. 2d, evaluated by Zeta potential characterization. The result shows the high zeta potential of the nanorods (0.01 g in 20 mL water, 25 °C) at 49 mV in water. This massive zeta potential of PANI nanorods could help form a stable colloidal suspension in water, which is vital for providing a way to disperse these conducting polymers in the water-base PU to fabricate high-performance ECAs. The dispersibility of PANI nanorods in various kinds of organic solvents is given in Fig. S3. It is found that PANIs could be dispersed well in many conventional organic solvents, meaning the possibility of being widely used to prepare various composites.

The PANI nanorods benefit from the rods-like nanostructures and exhibit significantly enhanced electrical conductivity than traditional PANI nanoparticles. The PANI nanorods have an electrical conductivity of 7.6 S cm^{-1}, which is approximately seven times higher than those of the PANI nanoparticles in other work [45–50]. Therefore, the enhanced conductivity and water dispersibility of these PANI nanorods could make PNAI nanorods work efficiently in high-performance ECAs using water-soluble resins.

The conductivity of PANI nanorods/WPU and PANI particles/WPU nanocomposites as a function of PNAI loading is investigated in Fig. 2e. The electrical conductivity of all the nanocomposites increases continuously with increasing PANI contents. As expected, the PANI nanorods/WPU nanocomposites have a much higher conductivity (20 S/m) and a lower percolation threshold (7 wt%) than those of the PANI particles/WPU nanocomposites, which is mainly due to the high conductivity of PANI nanorods and excellent dispersion ability in WPU resin.

Thus, PANI nanorods with high conductivity and high dispersion ability in the water-soluble resin are successfully obtained. These nanorods are expected to be favorable enhancers for the ECAs to improve conductivity and mechanical properties.

3.3 Electrical performance of the ECAs with water-soluble resins

To understand the effect of water-dispersible PANI nanorods on the conductivity of ECAs with water-soluble resins, two series of ECAs are prepared. ECAs composing silver flakes and PANI nanorods are named the WPN series (Table 1). The ECAs composing silver flakes only are named the WPU series (Table 1).

Figure 3a compares the resistivity of the WPN series ECAs and WPU series ECAs with various Ag loadings without heat treatment. The resistivity of the WPN-2 ECAs with a low level of Ag content (60%) reaches 2.1×10^{-5} Ω·cm, which is about 1/1500 of WPU-2 ECAs with the same Ag loading and even is 1/15 of WPU-3 ECAs with 70% Ag content. This result offers firm support that a small quantity of water-dispersible and highly conductive PANI nanorods can significantly enhance the conductivity of the ECAs based on water-soluble resin.

This substantial enhancement could be attributed to the successful formation of continuous conductive networks of silver flakes and PANI nanorods, confirmed by the cross-sectional SEM image of WPN-2 ECAs. As shown in Fig. S4, a large amount of PANI nanorods located between the gaps of the Ag flakes (in the red labeled region) are observed. It is evident that PANI nanorods could effectively connect Ag flakes in the composites of WPN-2 ECAs. Figure S5 shows a schematic representation for explaining the influence of PANI nanorods on the conductivity of the ECAs. For traditional ECAs, a substantial part of the total resistance comes from the tunnel resistance among the silver flakes of the ECAs. These resistances could be significantly reduced by adding highly conductive and dispersed PANI nanorods into the gaps among Ag flakes. These PANI could serve as conductive paths to connect neighboring silver flakes of ECAs.

Figure 3b shows the resistivity for WPN serials ECAs with different amounts of PANI nanorods. For the ECAs of WPU-2 without PANI nanorods, high resistivity is obtained at 2600×10^{-5} Ω·cm, which is higher than the ECAs previously reported due to the lower silver content and curing temperature [8, 51]. After adding a small number of PANI nanorods, the electrical resistivity of the ECAs drops sharply. When the PANI nanorods are raised further to 6 wt%, the resistivity of the ECAs decreases to an optimized value of 2.1×10^{-5} Ω·cm (WPN-2). Compared with other work using the ECAs reinforced conducting-polymers, the WPN-2 ECAs have a maximum effective conducting-polymer doping concentration (Table S1), indicating that water-dispersible PANI nanorods have a high dispersion in water-soluble composites.

Notably, WPN serial ECAs exhibits ultrahigh electrical conductivity with different cured temperatures (Fig. 3c). The resistivity of the ECAs decreases with elevated cured temperature, which is similar to other ECAs' systems [18, 25]. The ECAs prepared at room temperature show a reasonably low electrical resistivity (2.1×10^{-5} Ω·cm). These results show that the ECAs could be applied to flexible electronic devices that require low-temperature packaging and sealing techniques.
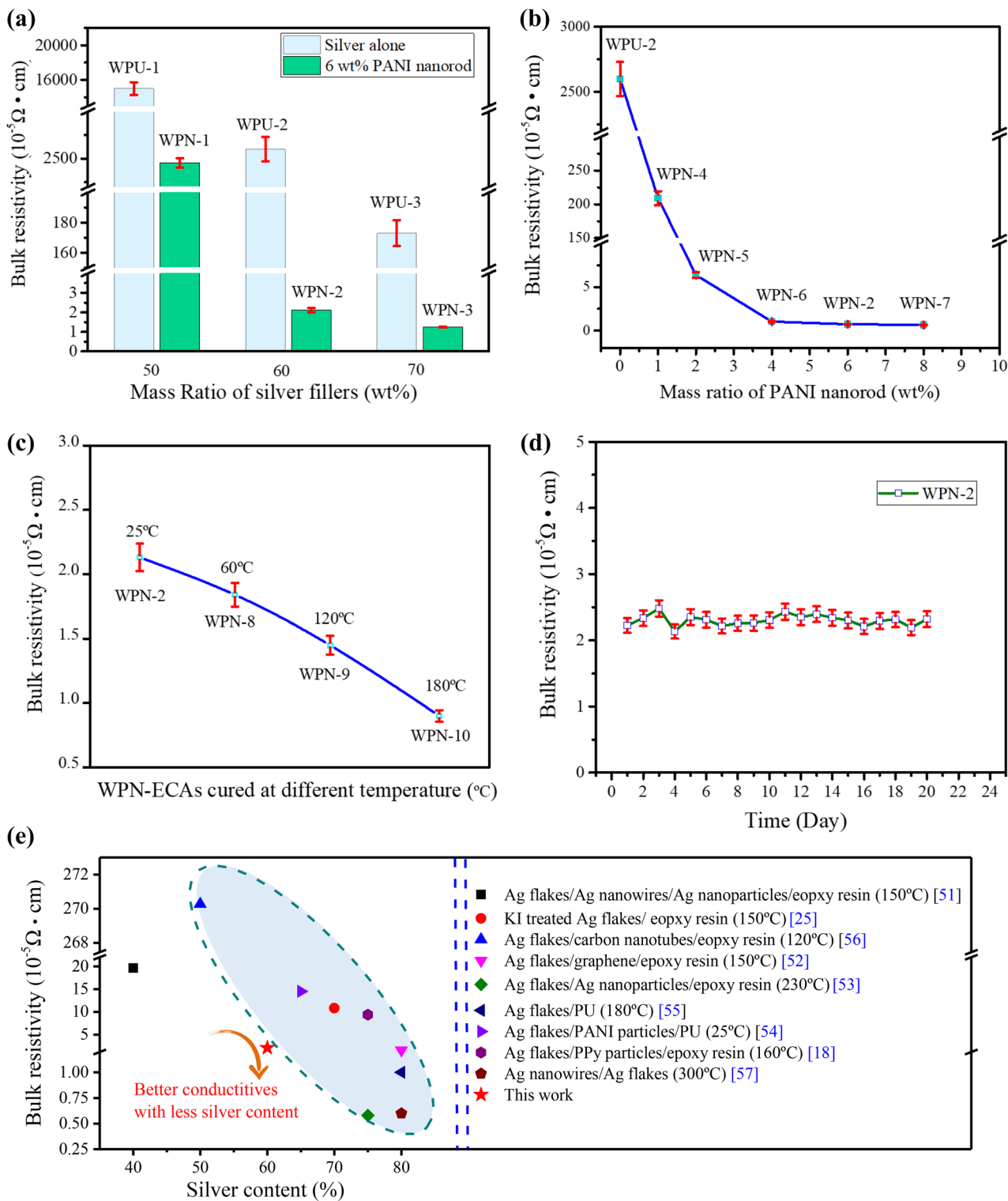
Fig. 3 **a** The bulk resistivity of the ECAs with different silver fillers loading. **b** The resistivity of WPN-ECAs with varying loading of PANI content. **c** The WPN-ECAs cured at different temperatures. **d** The electrical stability of WPN-2 ECAs with uninterrupted humidity-heat treatment. **e** The comparison of the electrical performances of the WPN serials ECAs with some works on high-performance ECAs
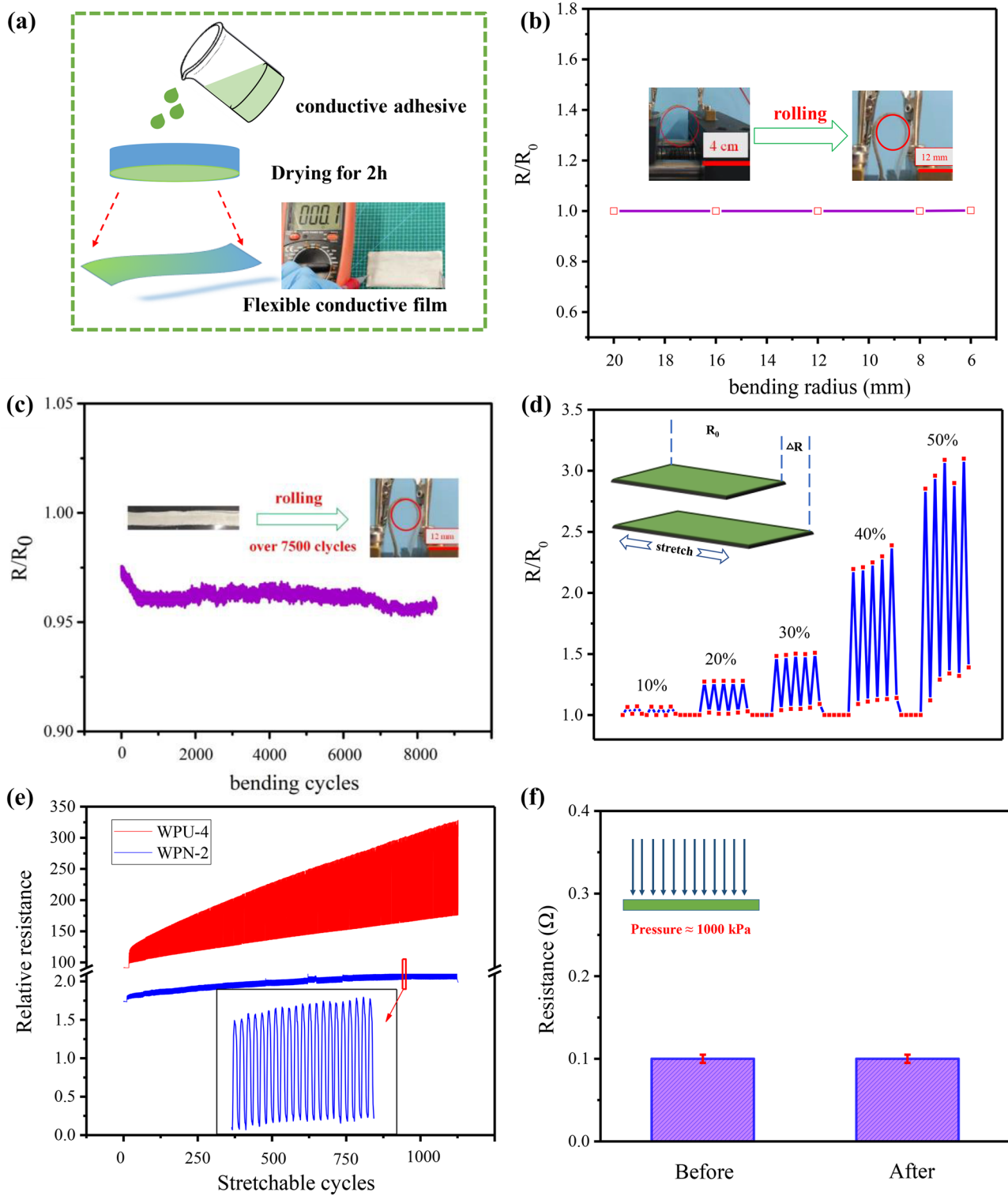
Fig. 4 **a** A schematic diagram for preparing the flexible conductive film. **b** The electrical performance of the films in the different bending status. **c** The durability of the conductive films with high bending status. **d** The resistance response of the films with various cyclic strain rates (10–50%) for 5 stretching cycles. **e** The durability of the conductive films with high stretchable status. **f** The resistance response of conductive films under high-pressure test

The WPN-2 ECA conductive film is aged at 80 °C and 65% relative humidity for 20 days to evaluate the stability (Fig. 3d). For WPN-2 ECA, the conductivity remains stable at 80 °C and 65% RH. This data displays that WPN-2 ECAs have excellent durability under uninterrupted humidity-heat treatment.

Figure 3e compares the electrical performances of the WPN-2 ECAs with some recent works on high-performance ECAs [18, 25, 51–57]. As displayed in Fig. 3e, the resistivity of WPN-2 ECAs (60 wt% Ag content, cured at 25 °C) exhibits an exceptionally low value of 2.1×10^{-5} $\Omega \cdot cm$, which is significantly lower than those of the most reported ECAs. Moreover, the water-based resin makes the ECAs more environmentally friendly because no volatile organic solvents are concerned. The preparation is also more energy-efficient because the curing of ECAs with heat possessing is not necessary. Therefore, the method proposed in this paper is particularly beneficial to help achieve the goal of manufacturing high-performance ECAs at a low cost.

3.4 Electrical performance of PANI-reinforcement flexible conductive film under mechanical deformation

In the past few years, considerable progress has been made in the field of flexible electronics. Flexible electronics, specifically those dedicated to the fabrication of conductors, sensors, or printed circuits on flexible and stretchable substrates, need further development to keep their electrical performance under mechanical deformation [58, 59]. Herein, we introduce a kind of flexible conductive film made by WPN-2 ECAs with excellent electrical stability in bending and stretching conditions.

Figure 4a shows a schematic diagram for preparing the flexible conductive film ($100 \times 50 \times 0.05$ mm) with a low resistance of 0.1 Ω by the casting method. Figure 4b gives the electrical performance of conductive films in the different bending states, defined as a series of the bending radius. For the conductive films, even when bent to the smallest bending radius of 6 mm using our experimental instrument, almost no changes of resistance are noticed (change is smaller than $\pm 5\%$). Furthermore, the resistance remains almost unchanged during more than 8000 cycles of bending to a small radius of 6 mm (Fig. 4c).

The film's stretchable electrical performance is another critical property for flexible electronics. Figure 4d shows the resistance response of the films with various cyclic strain rates (10–50%) for 5 stretching cycles. The conductive films have a stable electrical performance in the different stretch statuses. The film shows excellent tensile elongation at a break of more

Fig. 5 Application of the ECAs (WPN-2) for printed circuits. **a** The circuits with a width of 2 mm. **b** The circuits under a highly bend state. **c** An alternating blinking LED device based on the printed circuits. **d** The device could keep stable operation under a high bending condition
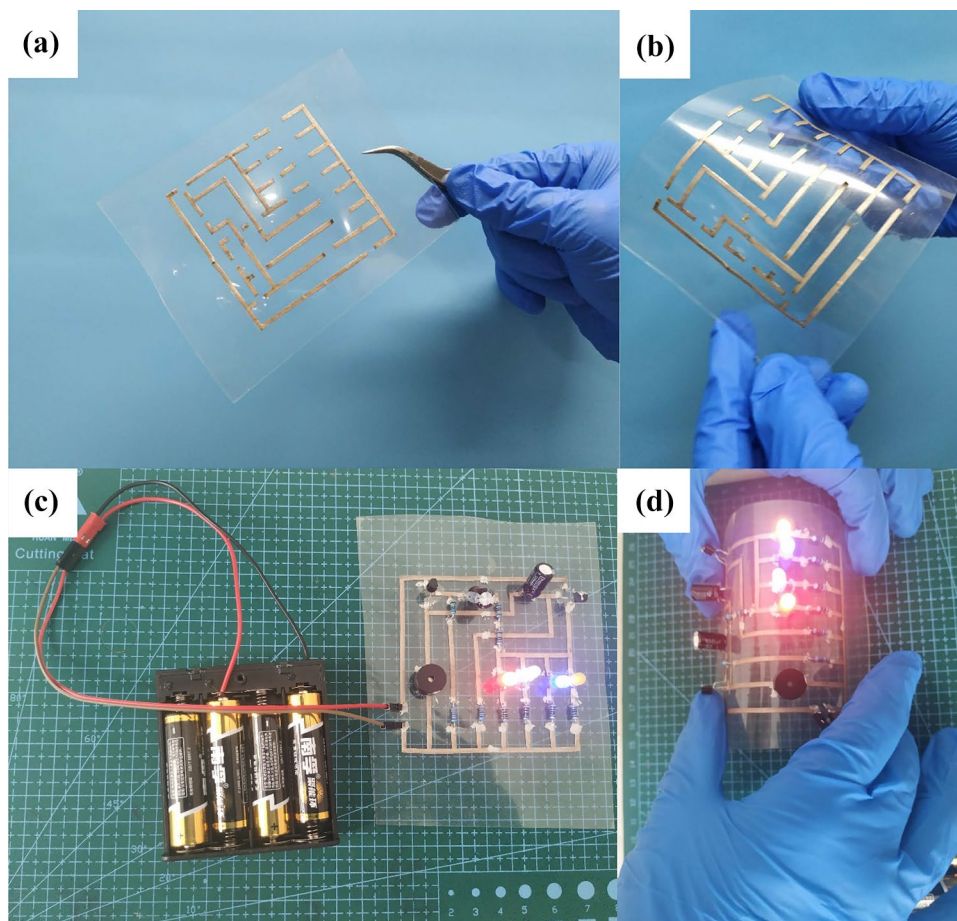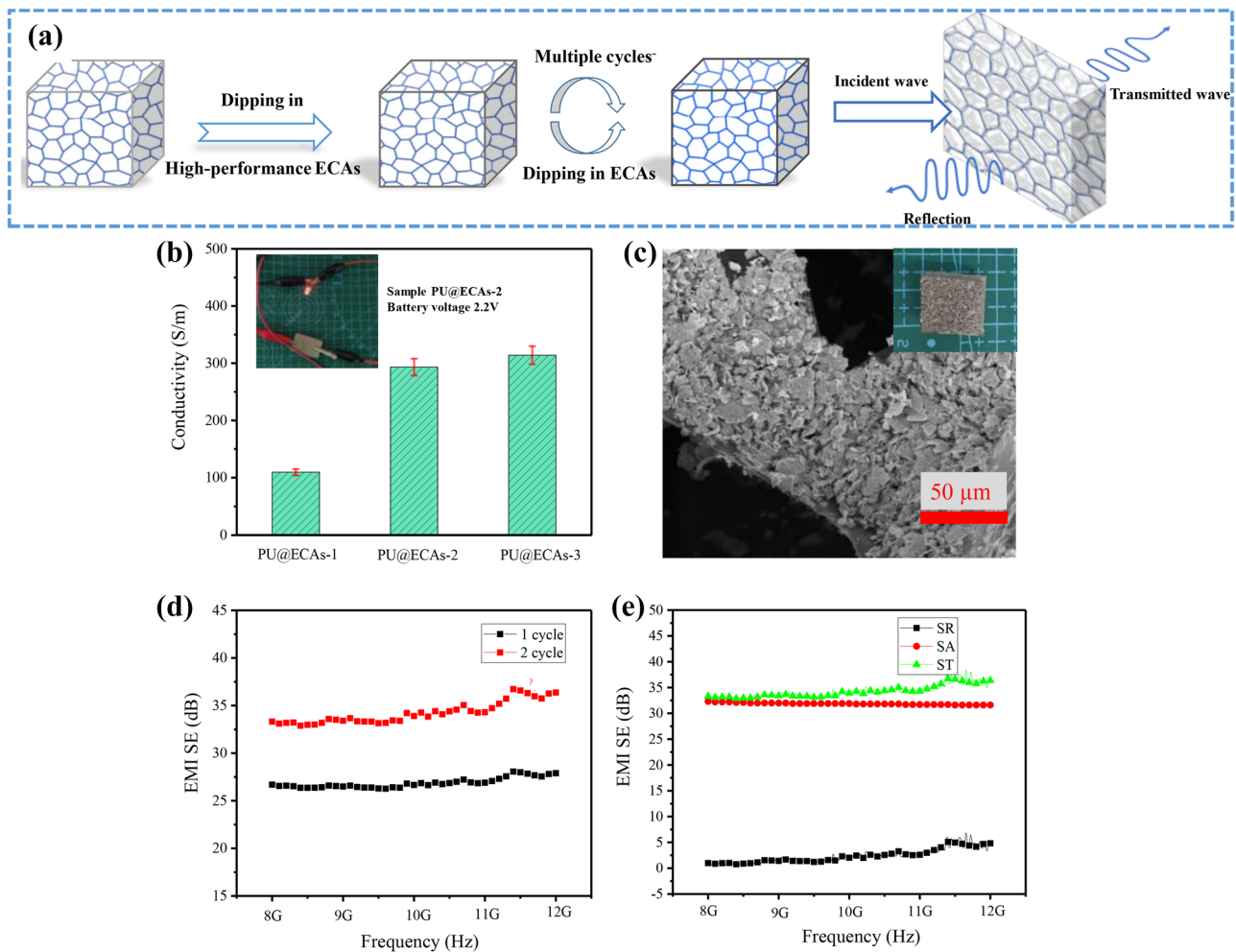
Fig. 6 a The schematic fabricating procedure of conductive PU sponges. **b** The conductivity of the foams with different dipping cycles; the inset shows that the foam could serve as a conductor to drive a light-emitting diode (LED). **c** The SEM images of the foams (PU@ECAs-2); the inset shows the macro morphology of the foam. **d** The EMI shielding properties of the conductive foam with various dipping cycles. **e** SE total (ST), SE$_A$ (SA), and SE$_R$ (SR) of the conductive foams with two dipping cycles

than 300% in Fig. S6. No noticeable resistance changes with more significance than ± 10% are observed in the conductive films stretched to 120% for more than 1000 cycles.

In contrast, apparent variation with 400% changes in the resistance of the conductive films (WPU-4) without PANIs is observed in Fig. 4e. Moreover, the resistance of the conductive films (The reduced thickness is about 100 μm, which is about 1/5 its original thickness) remains stable under 1000 kPa pressure (Fig. 4f). These results show that the conductive film produced by WPN-2 ECAs could exhibit outstanding electrical performances with different modes of mechanical deformation, which is crucial for flexible electronic devices.

3.5 Applications of the ECAs for printed circuits

To illustrate the applications of the ECAs for printed electronics, a printed circuit with a width of 2 mm produced by WPN-2 ECAs is shown. Figure 5a, b show flexibility and good adhesion of the printed circuits. The specific adhesion performance of the ECAs is shown in Fig. S7. An alternating blinking LED device based on the printed circuits is displayed in Fig. 5c. Figure 5d illustrates the stable operating state of the device under a highly bend condition.

3.6 Applications of the ECAs for high-performance electromagnetic interference shielding devices

To further expand the application range of ECAs for flexible electronics, light-weight and extraordinarily conductive PU sponges are innovatively manufactured for electromagnetic interference shielding (EMI) applications with high-performance WPN-2 ECAs and flexible PU foams. As is well known, the EMI SE of the conductive PU sponge mainly depends on the conductive filler's inherent conductivity and

connectivity [60, 61]. We propose that high-performance conductive adhesives could form a high-quality conductive path on the insulating PU foam through a simple impregnation process due to its good conductivity and adhesion. In this way, high-performance shielding materials with excellent conductivity and EMI SE at a low cost can be obtained.

Figure 6a displays the schematic fabricating procedure of conductive PU sponges. The commercial PU sponges are dip-coated with the ECA suspension for different cycles to fabricate high-performance EMI devices. In Fig. 6b, the foams' conductivity with varying dipping cycles is plotted. The conductivity of the foam sharply increases with the cycle numbers. With only two cycles, the foam shows excellent conductivity of 293 S/m^{-1}, which is vital for fabricating electromagnetic interference shielding devices. Also, the foam with such a high conductivity could serve as a conductor to drive a light-emitting diode (LED) with the power of 1.5 W. The SEM image of the foams (PU@ECAs-2) is shown in Fig. 6c. It can be observed that the silver flakes gather together and stick to the surface of the skeleton of the foam. This morphology makes it reasonable to obtain a high electrical conductivity to fabricate electromagnetic interference shielding devices.

The EMI shielding properties of the conductive foam with various dipping cycles are evaluated in the X band (8.2–12.4 GHz) in Fig. 6d. The conductive foam shows very high EMI SE, even only dipping one cycle. The EMI SE of the foam (one cycle) can exceed 25 dB, which can meet the requirement of most shielding applications of smart electronic devices [62, 63]. By improving the number of cycles, the EMI SE value can be further improved to 34 dB. The conductive foams with two cycles are chosen as examples to illustrate the contribution from the absorption (SE$_A$) and reflection (SE$_R$) to the total SE (SE total) in the X band. As shown in Fig. 6e, the significant contribution toward SE total is SE$_A$, which means that most of the energy loss of electromagnetic waves by passing through the shielding material is absorption losses.

4 Conclusion

In summary, we reported new high-performance ECAs as printed conductive materials for flexible conductive films, printed circuits, and electromagnetic interference shielding devices. Only a small amount of the water-dispersible PANI nanorods (6%) can enable gap-filling among Ag flakes in WPU resins, and thus, the ECAs showed ultralow electrical resistivity (2.1×10^{-5} Ω·cm). Due to its highly conductive and environmentally benign character, the ECAs could exhibit elegant versatility for flexible electronics. We demonstrated their potentials in flexible conductive films,

printed circuits, and electromagnetic interference shielding devices. The conductivity of the films remained unchanged under highly mechanical deformation. The printed circuits have excellent flexibility and good adhesion on the flexible substrate. Besides, electromagnetic interference shielding devices have remarkable electromagnetic interference shielding effectiveness for shielding applications of smart electronic devices. We expect that these high-performance ECAs can fit the requirements of not only traditional electronic packaging but also the new areas for various flexible electronic devices.

Declarations

Competing interests The authors declare no competing interests.

References

1. Yang C, Wong CP, Yuen MMF (2013) Printed electrically conductive composites: conductive filler designs and surface engineering. J Mater Chem C 1(26):4052–4069

2. Janeczek K (2020) Composite materials for printed electronics in Internet of Things applications. Bull Mater Sci 43:1–10

3. Lee B, Han H, Hahn H-G, Doh JM, Park S-H, Lee E, Lee S-S, Park C, Lim HS, Lim JA (2020) Ecofriendly catechol lipid bioresin for low-temperature processed electrode patterns with strong durability. ACS Appl Mater Interfaces 12(14):16864–16876

4. Song B, Wang X, Patel S, Wu F, Moon K-S, Wong C-P (2020) Flexible and electrically conductive composites based on 3D hierarchical silver dendrites. Soft Matter

5. Yan Q, Zhou M, Fu H (2020) A reversible and highly conductive adhesive: towards self-healing and recyclable flexible electronics. J Mater Chem C 8(23):7772–7785

6. Sun Q, Qian B, Uto K, Chen J, Liu X, Minari T (2018) Functional biomaterials towards flexible electronics and sensors. Biosens Bioelectron 119:237–251

7. Gu H, Ma C, Gu J, Guo J, Yan X, Huang J, Zhang Q, Guo Z (2016) An overview of multifunctional epoxy nanocomposites. J Mater Chem C 4(25):5890–5906

8. Chen Y, Li Q, Li C, Dai Z, Yan H, Zhu M, Zhang Y, Yao Y, Li Q (2020) Regulation of multidimensional silver nanostructures for high-performance composite conductive adhesives. Compos. A:Appl. Sci. Manuf. 137:106025

9. Wen J, Tian Y, Hang C, Zheng Z, Zhang H, Mei Z, Hu X, Tian Y (2019) Fabrication of novel printable electrically conductive adhesives (ECAs) with excellent conductivity and stability enhanced by the addition of polyaniline nanoparticles. Nanomaterials 9(7):960

10. Cao G, Gao X, Wang L, Cui H, Lu J, Meng Y, Xue W, Cheng C, Tian Y, Tian Y (2019) Easily synthesized polyaniline@ cellulose nanowhiskers better tune network structures in Ag-based adhesives: Examining the improvements in conductivity, stability, and flexibility. Nanomaterials 9(11):1542

11. Cao G, Hao C, Gao X, Lu J, Xue W, Meng Y, Cheng C, Tian Y (2019) Carbon nanotubes with carbon blacks as cofillers to improve conductivity and stability. ACS Omega 4(2):4169–4175

12. Ko Y, Oh J, Park KT, Kim S, Huh W, Sung BJ, Lim JA, Lee S-S, Kim H (2019) Stretchable conductive adhesives with superior electrical stability as printable interconnects in washable textile electronics. ACS Appl Mater Interfaces 11(40):37043–37050

13. Messina E, Leone N, Foti A, Di Marco G, Riccucci C, Di Carlo G, Di Maggio F, Cassata A, Gargano L, D'Andrea C (2016) Double-wall nanotubes and graphene nanoplatelets for hybrid conductive adhesives with enhanced thermal and electrical conductivity. ACS Appl Mater Interfaces 8(35):23244–23259

14. Secor EB, Gao TZ, Islam AE, Rao R, Wallace SG, Zhu J, Putz KW, Maruyama B, Hersam MC (2017) Enhanced conductivity, adhesion, and environmental stability of printed graphene inks with nitrocellulose. Chem Mater 29(5):2332–2340

15. Ma H, Ma M, Zeng J, Guo X, Ma Y (2016) Hydrothermal synthesis of graphene nanosheets and its application in electrically conductive adhesives. Mater Lett 178:181–184

16. Cao G, Wang L (2020) Tian Y (2020) Highly dispersed polypyrrole nanotubes for improving the conductivity of electrically conductive adhesives. J Mater Sci Mater Electron 31:9675–9684

17. Si P, Trinidad J, Chen L, Lee B, Chen A, Persic J, Lyn R, Leonenko Z, Zhao B (2018) PEDOT: PSS nano-gels for highly electrically conductive silver/epoxy composite adhesives. J Mater Sci Mater Electron 29(3):1837–1846

18. Wen J, Tian Y, Mei Z, Wu W, Tian Y (2017) Synthesis of polypyrrole nanoparticles and their applications in electrically conductive adhesives for improving conductivity. RSC Adv 7(84):53219–53225

19. Cao G, Cui H, Wang L, Wang T, Tian Y (2020) Highly conductive and highly dispersed polythiophene nanoparticles for fabricating high-performance conductive adhesives. ACS Appl Electron Mater 2(9):2750–2759

20. Zhang Y, Zhu P, Li G, Cui Z, Cui C, Zhang K, Gao J, Chen X, Zhang G, Sun R (2019) PVP-mediated galvanic replacement synthesis of smart elliptic Cu–Ag nanoflakes for electrically conductive pastes. ACS Appl Mater Interfaces 11(8):8382–8390

21. Ren H-M, Guo Y, Huang S-Y, Zhang K, Yuen MMF, Fu X-Z, Yu S, Sun R, Wong C-P (2015) One-step preparation of silver hexagonal microsheets as electrically conductive adhesive fillers for printed electronics. ACS Appl Mater Interfaces 7(24):13685–13692

22. Ma H, Yin G, Yan S, Li Z, Ma Y, Ma L (2018) Highly conductive and stretchable Ag nanodendrite-based composites for application in nanoelectronics. ACS Appl Nano Mater 2(1):351–359

23. Matsuhisa N, Inoue D, Zalar P, Jin H, Matsuba Y, Itoh A, Yokota T, Hashizume D, Someya T (2017) Printable elastic conductors by in situ formation of silver nanoparticles from silver flakes. Nat Mater 16(8):834–840

24. Tseng L-T, Jhang R-H, Ho J-Q, Chen C-H (2019) Molecular approach to enhance thermal conductivity in electrically conductive adhesives. ACS Appl Electron Mater 1(9):1890–1898

25. Li C, Li Q, Long X, Li T, Zhao J, Zhang K, E S, Zhang J, Li Z, Yao Y, (2017) In situ generation of photosensitive silver halide for improving the conductivity of electrically conductive adhesives. ACS Appl Mater Interfaces 9(34):29047–29054

26. Li C, Li Q, Cheng L, Li T, Lu H, Tang L, Zhang K, Songfeng E, Zhang J, Li Z (2017) Conductivity enhancement of polymer composites using high-temperature short-time treated silver fillers. Compos Part A Appl Sci Manuf 100:64–70

27. Li C, Gong X, Tang L, Zhang K, Luo J, Ling L, Pu J, Li T, Li M, Yao Y (2015) Electrical property enhancement of electrically conductive adhesives through Ag-coated-Cu surface treatment by terephthalaldehyde and iodine. J Mater Chem C 3(24):6178–6184

28. Bhattacharjee S (2016) DLS and zeta potential–what they are and what they are not? J Control Release 235:337–351

29. Zhuang Z, Wang W, Wei Y, Li T, Ma M, Ma Y (2021) Preparation of polyaniline nanorods/manganese dioxide nanoflowers core/shell nanostructure and investigation of electrochemical performances. Compos Hybrid Mater Adv. https://doi.org/10.1007/s42114-021-00225-0

30. Liao G, Li Q, Xu Z (2019) The chemical modification of polyaniline with enhanced properties: a review. Prog Org Coat 126:35–43

31. Jangid NK, Jadoun S, Kaur N (2020) A review on high-throughput synthesis, deposition of thin films and properties of polyaniline. Eur Polym J 125:109485

32. Li S, Yang C, Sarwar S, Nautiyal A, Zhang P, Du H, Liu N, Yin J, Deng K, Zhang X (2019) Facile synthesis of nanostructured polyaniline in ionic liquids for high solubility and enhanced electrochemical properties. Adv Compos Hybrid Mater 2(2):279–288

33. Hu Q, Zhou J, Qiu B, Wang Q, Song G, Guo Z (2021) Synergistically improved methane production from anaerobic wastewater treatment by iron/polyaniline composite. Adv Compos Hybrid Mater 4(2):265–273

34. Baker CO, Huang X, Nelson W, Kaner RB (2017) Polyaniline nanofibers: broadening applications for conducting polymers. Chem Soc Rev 46(5):1510–1525

35. Ma Y, Zhuang Z, Ma M, Yang Y, Li W, Lin J, Dong M, Wu S, Ding T, Guo Z (2019) Solid polyaniline dendrites consisting of high aspect ratio branches self-assembled using sodium lauryl sulfonate as soft templates: synthesis and electrochemical performance. Polymer 182:121808

36. Ma Y, Ma M, Yin X, Shao Q, Lu N, Feng Y, Lu Y, Wujcik EK, Mai X, Wang C, Guo Z (2018) Tuning polyaniline nanostructures via end group substitutions and their morphology dependent electrochemical performances. Polymer 156:128–135

37. Ingle RV, Shaikh SF, Pankaj KÂ, Bhujbal Pankaj KÂ, Pathan HM, Tabhane VA (2020) Polyaniline doped with protonic acids: optical and morphological studies. ES Materials & Manufacturing 8:54–59

38. Xu X, Fu Q, Gu H, Guo Y, Zhou H, Zhang J, Pan D, Wu S, Dong M, Guo Z (2020) Polyaniline crystalline nanostructures dependent negative permittivity metamaterials. Polymer 188:122129

39. Bláha M, Trchová M, Bober P, Morávková Z, Prokeš J, Stejskal J (2017) Polyaniline: aniline oxidation with strong and weak oxidants under various acidity. Mater Chem Phys 194:206–218

40. Jeong S, Cho H, Han S, Won P, Lee H, Hong S, Yeo J, Kwon J, Ko SH (2017) High efficiency, transparent, reusable, and active PM2. 5 filters by hierarchical Ag nanowire percolation network. Nano Lett 17(7):4339–4346

41. Kazemi Y, Kakroodi AR, Ameli A, Filleter T, Park CB (2018) Highly stretchable conductive thermoplastic vulcanizate/carbon nanotube nanocomposites with segregated structure, low percolation threshold and improved cyclic electromechanical performance. J Mater Chem C 6(2):350–359

42. Trchová M, Stejskal J (2011) Polyaniline: the infrared spectroscopy of conducting polymer nanotubes (IUPAC Technical Report). Pure Appl Chem 83(10):1803–1817

43. Sapurina I, Li Y, Alekseeva E, Bober P, Trchova M, Moravkova Z, Stejskal J (2017) Polypyrrole nanotubes: the tuning of morphology and conductivity. Polymer 113:247–258

44. Stejskal J (2020) Interaction of conducting polymers, polyaniline and polypyrrole, with organic dyes: polymer morphology control, dye adsorption and photocatalytic decomposition. Chem. Pap:1–54

45. Li ZF, Swihart MT, Ruckenstein E (2004) Luminescent silicon nanoparticles capped by conductive polyaniline through the self-assembly method. Langmuir 20(5):1963–1971. https://doi.org/10.1021/la0358926

46. Hu W, Chen S, Yang Z, Liu L, Wang H (2011) Flexible electrically conductive nanocomposite membrane based on bacterial cellulose and polyaniline. J Phys Chem B 115(26):8453–8457

47. Cho MS, Park SY, Hwang JY, Choi HJ (2004) Synthesis and electrical properties of polymer composites with polyaniline nanoparticles. Mater Sci Eng C 24(1–2):15–18

48. Fu GD, Zhao JP, Sun YM, Kang ET, Neoh KG (2007) Conductive hollow nanospheres of polyaniline via surface-initiated atom transfer radical polymerization of 4-vinylaniline and oxidative graft copolymerization of aniline. Macromolecules 40(6):2271–2275. https://doi.org/10.1021/ma0613988

49. Wang Y, Shi Y, Xu X, Liu F, Yao H, Zhai G, Hao J, Li G (2009) Preparation of PANI-coated poly (styrene-co-styrene sulfonate) nanoparticles in microemulsion media. Colloids Surf A Physicochem Eng Asp 345(1–3):71–74

50. Zhou Q, Wang J, Ma Y, Cong C, Wang F (2007) The relationship of conductivity to the morphology and crystallinity of polyaniline controlled by water content via reverse microemulsion. Colloid Polym Sci 285(4):405–411

51. Ji Y-H, Liu Y, Huang G-W, Shen X-J, Xiao H-M, Fu S-Y (2015) Ternary Ag/epoxy adhesive with excellent overall performance. ACS Appl Mater Interfaces 7(15):8041–8052

52. Amoli BM, Trinidad J, Rivers G, Sy S, Russo P, Yu A, Zhou NY, Zhao B (2015) SDS-stabilized graphene nanosheets for highly electrically conductive adhesives. Carbon 91:188–199

53. Jiang H, Moon K-s, Li Y, Wong CP (2006) Surface functionalized silver nanoparticles for ultrahigh conductive polymer composites. Chem Mater 18(13):2969–2973

54. Wen J, Tian Y, Hao C, Wang S, Mei Z, Wu W, Lu J, Zheng Z, Tian Y (2019) Fabrication of high performance printed flexible conductors by doping of polyaniline nanomaterials into silver paste. J Mater Chem C 7(5):1188–1197

55. Li Z, Zhang R, Moon KS, Liu Y, Hansen K, Le T, Wong CP (2013) Highly conductive, flexible, polyurethane-based adhesives for flexible and printed electronics. Adv Funct Mater 23(11):1459–1465

56. Luo J, Cheng Z, Li C, Wang L, Yu C, Zhao Y, Chen M, Li Q, Yao Y (2016) Electrically conductive adhesives based on thermoplastic polyurethane filled with silver flakes and carbon nanotubes. Compos Sci Technol 129:191–197

57. Zhang ZX, Chen XY, Xiao F (2011) The sintering behavior of electrically conductive adhesives filled with surface modified silver nanowires. J Adhes Sci Technol 25(13):1465–1480

58. Huang S, Liu Y, Zhao Y, Ren Z, Guo CF (2019) Flexible electronics: stretchable electrodes and their future. Adv Funct Mater 29(6):1805924

59. Chen X, Rogers JA, Lacour SP, Hu W, Kim D-H (2019) Materials chemistry in flexible electronics. Chem Soc Rev 48(6):1431–1433

60. Wu H, Zhong Y, Tang Y, Huang Y, Liu G, Sun W, Xie P, Pan D, Liu C, Guo Z (2021) Precise regulation of weakly negative permittivity in CaCu3Ti4O12 metacomposites by synergistic effects of carbon nanotubes and grapheme. Adv Compos Hybrid Mater. https://doi.org/10.1007/s42114-021-00378-y

61. Gu H, Xu X, Cai J, Wei S, Wei H, Liu H, Young DP, Shao Q, Wu S, Ding T (2019) Controllable organic magnetoresistance in polyaniline coated poly (p-phenylene-2, 6-benzobisoxazole) short fibers. ChemComm 55(68):10068–10071

62. Bagotia N, Choudhary V, Sharma DK (2019) Synergistic effect of graphene/multiwalled carbon nanotube hybrid fillers on mechanical, electrical and EMI shielding properties of polycarbonate/ethylene methyl acrylate nanocomposites. Compos B Eng 159:378–388

63. Sankaran S, Deshmukh K, Ahamed MB, Pasha SKK (2018) Recent advances in electromagnetic interference shielding properties of metal and carbon filler reinforced flexible polymer composites: a review. Compos Part A Appl Sci Manuf 114:49–71